178

in "Tantalum", TMS-AIME, 1996

LASALVIA et al

HIGH-STRAIN, HIGH-STRAIN-RATE RESPONSE OF ANNEALED AND SHOCKED TANTALUM

J.C. LaSalvia[a], Y.J. Chen[b], M.A. Meyers[ab], V.F. Nesterenko[b], M.P. Bondar[c], and Y.L. Lukyanov[c]

[a] Institute for Mechanics and Materials, Department of Applied Mechanics and Engineering Sciences, UC San Diego, La Jolla, CA 92093. [b] Department of Applied Mechanics and Engineering Sciences, UC San Diego, La Jolla, CA 92093. [c] Lavrentyev Institute of Hydrodynamics, Russian Academy of Sciences, Novosibirsk, 630090, Russia.

Abstract

Tantalum specimens of tubular geometry were subjected to large plastic shear strains (up to 1000%) at strain rates greater than 10^5 s^{-1} during their quasi-uniform collapse (partial) by explosively-generated energy (i.e. thick-walled cylinder method). Experiments were performed on annealed and pre-shocked (45 GPa peak pressure and 1.8 μs pulse duration) tantalum. Optical microscopy revealed distinct features on specimen cross-sections: (1) profuse ductile cracks initiated at the inner surface surrounded by regions of highly deformed grains; (2) regions ahead of the crack-tips which do not exhibit the elongated grain morphology; (3) large statically recrystallized grains at the inner surface; (4) diffuse shear bands running from the inner to outer surfaces; and (5) regions of highly deformed grains intermixed with slightly deformed grains. The diffuse appearance of the shear bands is believed due to the strong orientation dependence of the yield stress and subsequent anisotropy of the work-hardening behavior of the individual grains. The lower bound estimated temperature near the inner surface (macroscopic shear strain $\gamma > 10$), calculated using a modified Johnson-Cook constitutive equation, exceeds the recrystallization temperature as reported in the literature. Transmission electron microscopy revealed the following substructural features: (1) elongated dislocation cells ($\gamma < 2$, $T < 600$ K); (2) dislocation subgrains ($\gamma < 6$, $T < 800$ K); and (3) dynamically recrystallized micrograins ($\gamma < 8$, $T < 900$ K). The kinetics of static and dynamic recrystallization are correlated with the observed residual grain sizes. It is concluded that the observed dynamic recrystallization probably occurs by a rotational mechanism.

Introduction

Tantalum and tantalum-tungsten alloys, due to their high density and ductility, are attractive materials for use in anti-armor applications as explosively-forged projectiles (i.e. EFPs) or shaped charge liners[1,2]. Recently, Murr and co-workers characterized the microstructural changes in recovered shaped-charge[3,4] and EFP[5,6] specimens. Depending upon the location within the specimen, deformation microtwinning, dislocation cells, subgrains, and recrystallized grains were observed. Utilizing the thick-walled cylinder method[7-9], it is possible to simulate, in a controlled manner, the thermomechanical conditions that a material undergoes during shaped-charge or EFP processes (shear strains > 10 at strain-rates > 10^5 s^{-1}). Preshocking the material simulates the pressure pulse (generated by the detonation of the explosive) propagating through the EFP and shaped-charge prior to undergoing large plastic deformation. The results of this method applied to commercially pure tantalum, as well as their analysis, are the subject of this paper.

Experimental Procedures

Commercially pure tantalum, supplied by Cabot Corporation, Boyertown, PA, was used in this investigation. Tubular specimens prepared from plates (8 mm long, 3 mm thick, and 5.5 mm inner radius) and tubes (70 mm long, 3.3 mm thick, and 7.875 mm inner radius)[10], were inserted into the experimental set-up schematically illustrated in Figure 1. As can be seen from this figure, the radial collapse of the tantalum specimens is driven by the impulsive motion of the copper cylinder which itself is derived from the detonation of a low-detonation velocity (~ 4 km/s) and low density (~ 1 g/cm^3) explosive. Optical and transmission electron microscopy (i.e. TEM) were conducted on the collapsed specimens to identify microstructural mechanisms leading to localization. Further information on the experimental procedures, material used, specimen geometry, and results is provided by Nesterenko et al.[10] and Meyers et al.[11].

The shock preconditioning was carried out by impacting the specimen, using a fixture in which reflected waves were captured by lateral and bottom momentum traps. This insured that the material was subjected to a single stress pulse with an amplitude of 45 GPa and a duration of 1.8 μs. Further information on the experimental fixture used is given by Meyers et al.[12] and Murr et al.[13]. The pre-shocking of the tantalum generated a microstructure with profuse twinning (see Figure 2).

Results and Discussion

Microstructural Observations

Figure 3 shows transverse cross-sectional views of the (a) annealed and (b) pre-shocked materials after collapse. The residual central orifice (0.5 - 2 mm radius) is due to either jetting along the central axis or to insufficient energy for complete collapse. Figure 4 is a partial cross-section showing more clearly the different microstructural features. Arrows indicate diffuse shear bands which connect the inner and outer surfaces. At the inner surface, ductile cracks can be seen to propagate along these shear bands. Figure 5 is a close-up of the inner surface region. Well-defined recrystallized grains (17 μm size compared with 31 μm in the as-received material) are evident near the inner surface. The regions between the cracks show a highly elongated grain structure while at the crack-tips, the grain structure appears more equiaxed. A close-up of a crack-tip region is shown in Figure 6. Microhardness measurements from the regions at the tip of the cracks, coupled with flow stress data from Meyers et al.[14] and Hall-Petch parameters obtained from Armstrong[15] and Zerilli and Armstrong[16] predict a grain size of 0.1 μm[10]. This indicates that these regions could be recrystallized during plastic deformation (i.e. dynamic recrystallization). The Vickers microhardness values as a function of distance from the inner surface for a collapsed specimen prepared from the tube material is shown in Figure 7. The curve marked A is for regions of highly

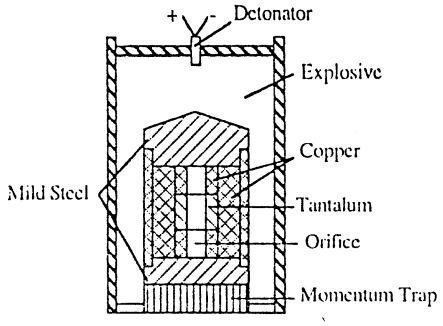

Figure 1 Schematic illustration of experiment set-up of "thick-walled cylinder" method.

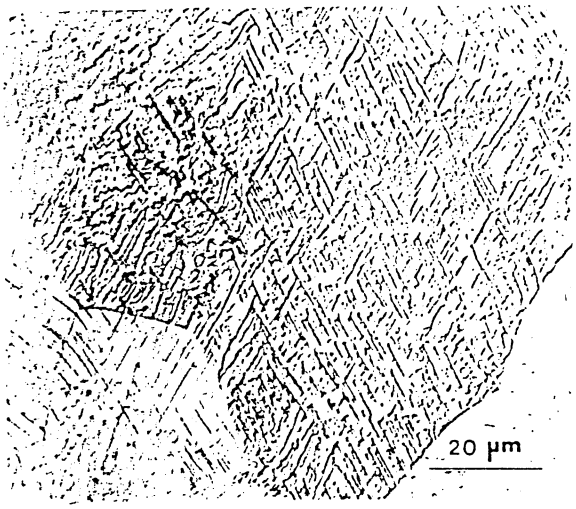

Figure 2 Profuse twinning produced within the shock loaded Ta.

elongated grains, while the curve marked B is for grains within these regions which were much less deformed. Figure 8 shows such a region. These microstructural features are believed to be formed due to the strong orientation dependences of the flow stress and work hardening behavior of single-crystal tantalum[17,18], as well as texture and thermal softening. During uniform collapse, the material is under a triaxial state of compression and individual grains become highly elongated due to the pure shear acting on them[10]. Obviously, those grains which are favorably oriented will experience a larger strain than those less favorably oriented. With increased deformation, these grains rotate such that their Schmid factors increase (i.e. texture softening) which leads to further localization. This is coupled with the anisotropy in the work hardening behavior observed in tantalum. Finally, the deformation becomes sufficiently large for the local temperature rise to cause a decrease in the flow stress which further enhances localization. The grains which were less favorably oriented are convected along due to compatibility constraints with these highly deformed grains.

Strain and Temperature Calculations

Based upon cylindrical geometry and constancy of volume, the effective ε_{eff} is given by[19]:

$$\varepsilon_{eff} = \left(\frac{2}{\sqrt{3}}\right)\varepsilon_r \qquad (1)$$

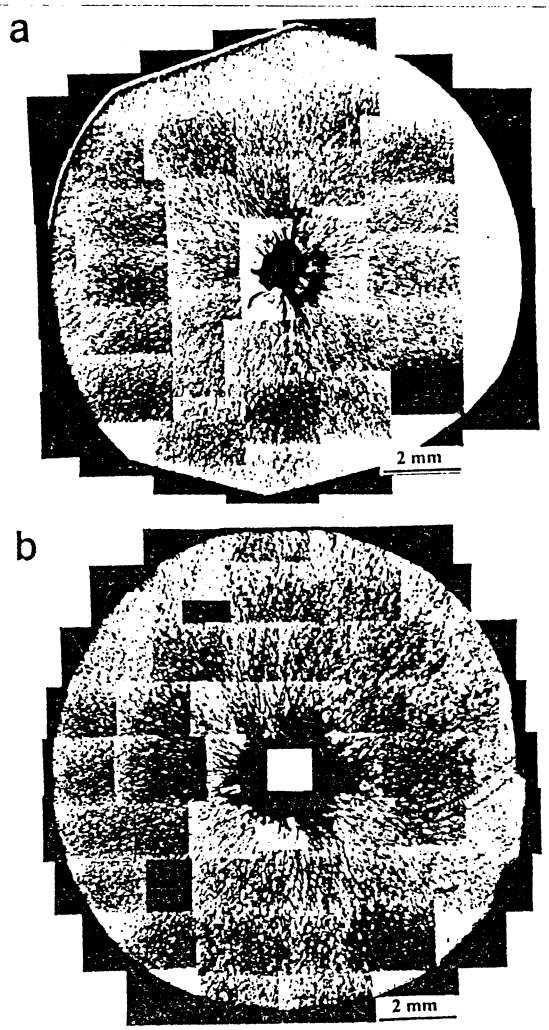

Figure 3 Cross-sectional view of a partially collapsed Ta tube after experiment: (a) without shock preconditioning; and (b) with shock preconditioning.

where ε_r, the radial true strain, is given by:

$$\varepsilon_r = \frac{1}{2}\ln\left(1 + \frac{a_o^2 - a^2}{r^2}\right) \qquad (2)$$

where a_o is the initial inner radius, a is the final inner radius, and r is the radius as measured in the final configuration.

The temperature rise in the specimens was calculated using a modified Johnson-Cook constitutive equation[10]. Assuming homogeneous deformation and 90% of the plastic work is converted into heat, the temperature rise as a function of strain, strain-rate, and test temperature is given by:

$$T = T_r + \frac{1}{\lambda}\ln\left\{e^{\lambda(T_o - T_r)} + 0.9\left(\frac{\lambda}{\rho C_p}\right)\left[1 + C\log\left(\frac{\dot{\varepsilon}}{\dot{\varepsilon}_o}\right)\right]\varepsilon\left(\sigma_o + \frac{B\varepsilon^n}{n+1}\right)\right\} \qquad (3)$$

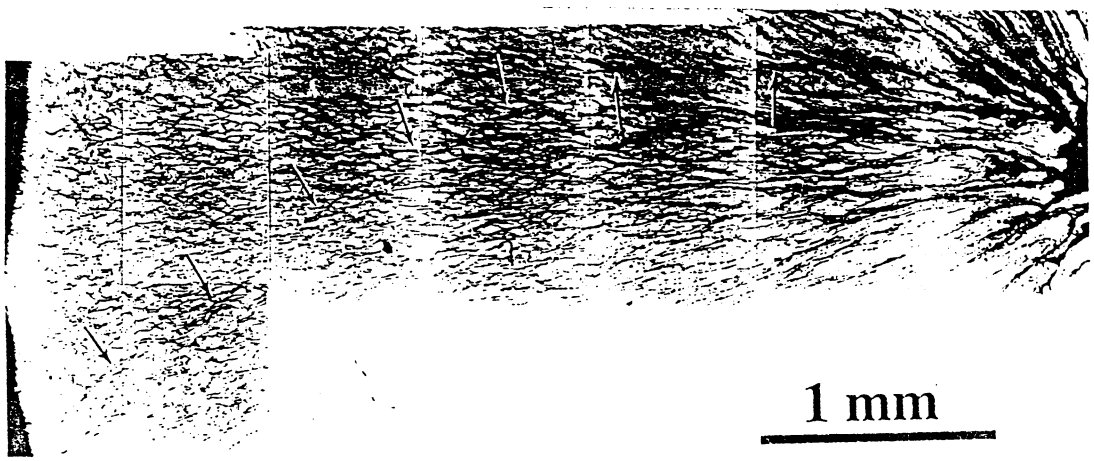

Figure 4 Partial transverse cross-section after an experiment.

Figure 5 Close-up of microstructural features near the inner surface.

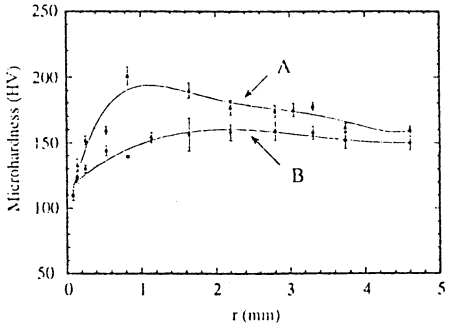

Figure 7 Variation of Vickers microhardness as a function of distance from the inner surface.

Figure 6 Microstructural features within the region surrounding the crack.

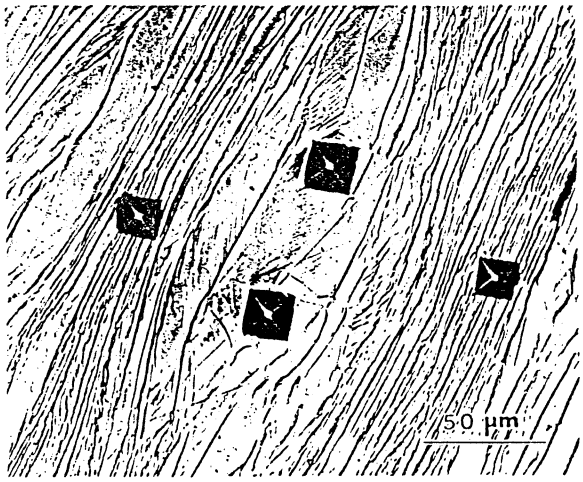

Figure 8 Localized deformation region exhibiting grains with differing amounts of elongation.

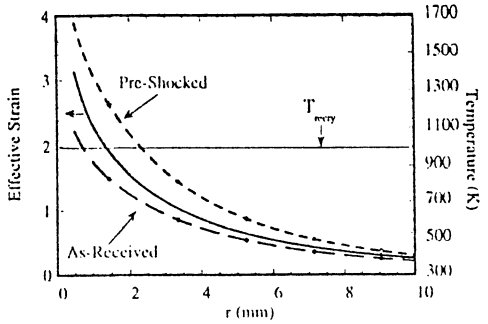

Figure 9 Effective strain and temperature distributions within the collapsed cylinder as given by Equations (1) and (3).

where σ_o = 684.5 MPa, B = 205.3 MPa, and n = 0.78 for the as-received material and σ_o = 820 MPa, B = 1388 MPa, and n = 0.84 for the pre-shocked material[13]. For both materials, C = 0.1, $\dot{\varepsilon}_o$ = 3.5 x 10^3 s^{-1}, T_r = 298 K, and λ = 1.4 x 10^{-3}[14]. Equations (1) and (3) are plotted in Figure 9. The temperature calculation was conducted with ε assumed constant and equal to the effective strain divided by the total deformation time (~ 8 μs[9]). Thus, at the inner surface, $\dot{\varepsilon} > 10^5$ s^{-1}. The heat capacity C_p was taken to be 140 J/kg*K[20]. The temperature range in which recrystallization has been observed is also marked in Figure 9. Köck and Paschen[21] measured temperatures in the 1200 - 1500 K range, while Beckenhauer et al.[22] measured a temperature of 1000 K for high purity tantalum heated at 800 K/s. Using 1000 K as a lower bound for recrystallization, from Figure 9, the recrystallized grain region is estimated to be approximately 0.5 mm wide. This is entirely consistent with microstructural observations (Figure 5) and microhardness measurements (Figure 7). The temperature rise for the pre-shocked material is larger than for the as-received material due to its higher yield stress and work-hardening rate.

It must be noted that Equation (3) does not take into account other possible heat sources in the vicinity of the central orifice such as jetting and compressed air. It must be further noted that the heat capacity C_p is weakly temperature dependent (C_p = 160 J/kg*K @ 1500 K)[20]. Therefore, the temperature estimation should be regarded as a lower bound for the true temperature.

Transmission Electron Microscopy Observations

Transmission electron microscopy was conducted to examine the evolution of the substructure with increasing strain. In general, the substructure evolves from isolated dislocations, to dislocation cells, to sub-grains with increasing misorientation (i.e. dynamic recovery), and finally to recrystallized micrograins. This sequence appears to be consistent with the earlier results obtained by Qiang et al.[2], Wittman et al.[23], Murr et al.[3-6], and Meyers et al.[14]. Figures 10(a) and 10(b) show elongated subgrains and their break-down into micrograins approximately 1.5 mm and 0.5 mm, respectively, from the central orifice. Note that the apparent size of the subgrains and micrograins is 0.1 - 0.2 μm, which is in agreement with the prediction based upon microhardness. It is apparent that the break-down of the elongated subgrains into the equiaxed micrograins is accomplished by a compatible rotation process. Gil Sevillano et al.[24] suggested that this process is the mechanism by which dynamic recrystallization occurs during high strain-rate deformation. Derby[25] analyzed rotation recrystallization, which is also discussed by Andrade et al.[26] for copper.

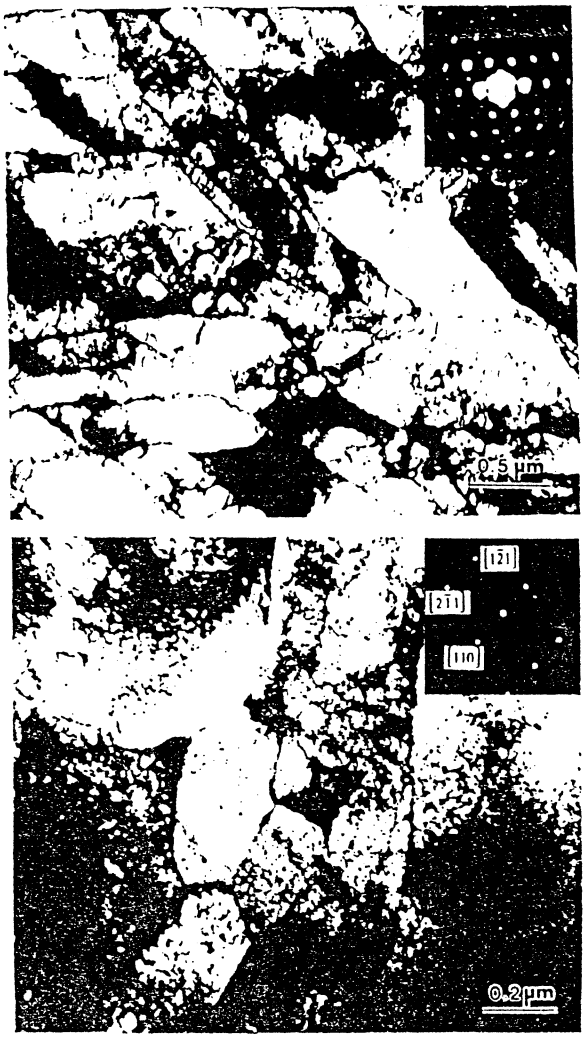

Figure 10 Break-down of elongated subgrains into micrograins: (a) 1.5 mm and (b) 0.5 mm from the central orifice.

Recrystallized Grain Size Analysis

As was mentioned previously, well-defined recrystallized grains were observed at the inner surface of the collapsed cylinders. Given that the grains are well-defined and fairly large, it is believed that they are mainly the result of post-deformation growth. Assuming that this is true, their size can be predicted using the simple steady-state grain growth equation[27]:

$$\Delta d = k_o \Delta t^{1/n} \exp\left(-\frac{Q}{2RT(t)}\right) \qquad (4)$$

where d is the instantaneous grain size, k_o is a rate constant, t is time, n is the growth exponent (which varies between 2 and 10 depending upon impurity content[27]), Q is the activation energy for the rate-controlling grain growth process, and T is the absolute temperature. The rate constant k_o and activation energy Q can be estimated from experimental results reported in the literature. Vandermeer and Snyder[17] reported the activation energy for self-diffusion to be equal to 394 kJ/mol. Krashechenko and

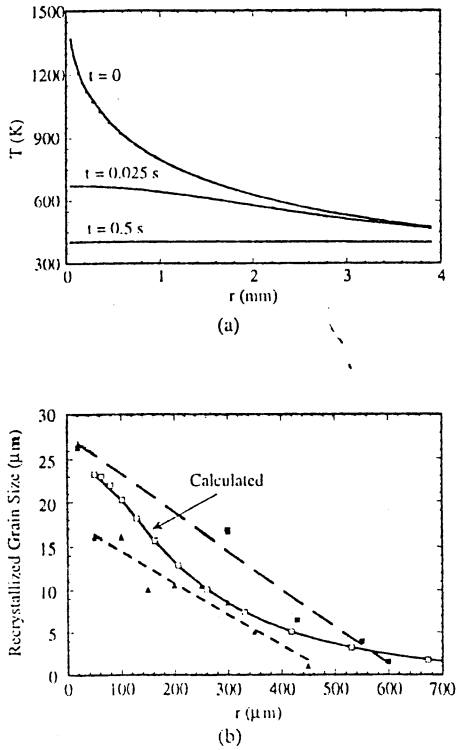

Figure 11 (a) Calculated temperature distribution within partially collapsed Ta tubes for several times. (b) Static recrystallized grain size estimate with n = 3.1.

Statsenko[28] reported the activation energy for plastic deformation occuring near half the melting temperature to be equal to 217 kJ/mol. Assuming Q to be equal to 300 kJ/mol, the rate constant k_n can be evaluated using the experimental result by Vandermeer and Snyder[17]; an annealing treatment at 1473 K for 7200 s resulted in a fully recrystallized grain size of 230 μm.

The functional time dependence of temperature, T(x,t), shown in Equation (4) was determined by conducting a heat transfer analysis on the collapsed cylinder, assuming that the initial temperature distribution is given by Equation (3). It was further assumed that the radius of the central orifice before unloading was 5×10^{-4} m. For this analysis, the thermal conductivity was taken to be equal to 60 W/m*K[29]. Figure 11(a) shows the spatial variation of the temperature within the cylinder for t = 0, 0.025, and 0.5 s. As can be seen, the temperature is essentially uniform after 0.5 s.

Substituting the temperature history determined from the heat transfer analysis into Equation (4) and then integrating over time yields the recrystallized grain size estimate. Figure 11(b) shows the results including the experimentally measured grain size. The best fit was obtained for n = 3.1, which corresponds to relatively pure material.

It is also possible to establish, using the above analysis, whether the fine recrystallized grains with sizes 0.1 - 0.2 μm, observed at the tips of the cracks (approximately 0.5 - 1.0 mm from inner surface) and only resolvable by TEM, could be produced by a migrational mechanism during plastic deformation. Based upon a deformation time of approximately 8 μs[9] and n = 3.1, the predicted recrystallized grain size is 0.01 μm. Thus, a migrational mechanism is highly unlikely and therefore, these grains were probably formed by a rotational mechanism.

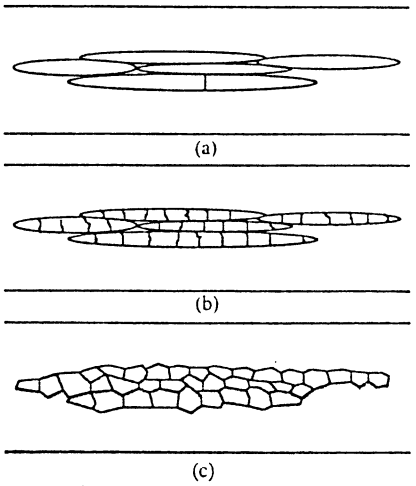

Figure 12 Microstructural evolution with plastic deformation: (a) elongated cells and subgrains; (b) break-up of subgrains; and (c) relaxed micrograin structure.

Conclusions

The thick-walled cylinder method was used to deform tantalum specimens at strain-rates > 10^5 s^{-1} to effective strains exceeding 3. The plastic strain increases logarithmically during collapse in this simple geometry. Another interesting feature of this technique is that the material's response to the deformation (i.e. shear localization) is not geometrically forced as it is in the hat-shaped specimen technique.

Optical and transmission electron microscopy reveal that the evolution of the microstructure consists of the formation of dislocations and dislocation cells, sub-grains (dynamic recovery), micrograins (dynamic recrystallization), and then large equiaxed grains (static recrystallization). Figure 12 illustrates the observed microstructural evolution. Profuse ductile cracking (propagating along shear localized regions) initiated at the inner surface. These cracks are evidence of residual tensile "hoop" stresses produced as a result of unloading.

The mechanism of localization appears to be dominated by the large orientation dependence of both the flow stress and work hardening behavior. This leads to texture softening. Favorably oriented grains localize first; however, further localization may become inhibited by surrounding grains which are less favorably oriented. Only after the shear stress is sufficiently large do these grains themselves localize. The result of which is a microstructure with both highly elongated grains and slightly elongated grains, which gives the appearance that the collapse process occurred uniformly.

Acknowledgements

This research was supported by the US Army Research Office under contract number DAAH-04-93-G-0261, as well as under its University Research Initiative Program (contract number DAAL-03-92-60108). Support by the National Science Foundation sponsored Institute for Mechanics and Materials is gratefully acknowledged.

References

1. M.J. Worswick, N. Qiang, P. Niessen, and R.J. Pick, "Microstructure and Fracture During High-Rate Forming of Iron and Tantalum," Shock-Wave and High-Strain-Rate Phenomena in Materials, eds. M.A. Meyers, L.E. Murr, and K.P. Staudhammer, (M. Dekker, NY, 1992), 87.

2. N. Qiang, P. Niessen, and R.J. Pick, "Dynamic-loading-induced Damage in Tantalum and Armco Iron," Materials Science & Engineering A (Structural Materials: Properties, Microstructure, and Processing), A160(1)(1993) 49-56.

3. A.C. Gurevitch, L.E. Murr, H.K. Shih, C.-S. Niou, A.H. Advani, D. Manuel, and L. Zernow, "Characterization and Comparison of Microstructures in the Shaped-Charge Regime: Copper and Tantalum," Materials Characterization, 30(3)(1993) 201-216.

4. H.K. Shih, L.E. Murr, C.-S. Niou, and L. Zernow, "Dynamic Recrystallization in a Tantalum Shaped Charge," Scripta Metallurgica et Materialia, 29(10)(1993) 1291-1296.

5. L.E. Murr, C.-S. Niou, and C. Feng, "Residual Microstructures in Explosively Formed Tantalum Penetrators," Scripta Metallurgica et Materialia, 31(1994) 297-302.

6. L.E. Murr, H.K. Shih, and C.-S. Niou, "Dynamic Recrystallization in Detonating Tantalum Shaped Charges: A Mechanism for Extreme Plastic Deformation," Materials Characterization, 33(1)(1994) 65-74.

7. V.F. Nesterenko, A.N. Lazaridi, and S.A. Pershin, "Localization of Deformation in Copper by Explosive Compression of Hollow Cylinders," Fizika Goreniya I Vzryva, 25(1989) 154-155.

8. V.F. Nesterenko, M.P. Bondar, and I.V. Ershov, "Instability of Plastic Flow at Dynamic Pore Collapse," High-Pressure Science and Technology-1993, eds. S.C. Schmidt, J.W. Shaner, G.A. Samara, and M. Ross, (AIP Press, NY, 1994), 1173-1176.

9. V.F. Nesterenko and M.P. Bondar, "Investigation of Deformation Localization by the "Thick-Walled Cylinder" Method," DYMAT J., 1 (1994) 245-251.

10. V.F. Nesterenko, M.A. Meyers, H.C. Chen, and J.C. LaSalvia, Materials Science & Engineering A (Structural Materials: Properties, Microstructure, and Processing), accepted (1996).

11. M.A. Meyers, V.F. Nesterenko, Y.J. Chen, J.C. LaSalvia, M.P. Bondar, and Y.L. Lukyanov, Metallurgical and Materials Applications of Shock-Wave and High-Strain-Rate Phenomena, eds. L.E. Murr, K.P. Staudhammer, and M.A. Meyers, (Elsevier, NY, 1995), 487.

12. M.A. Meyers, U.R. Andrade, and A.H. Chokshi, "The Effect of Grain Size on the High-Stran, High-Strain-Rate Behavior of Copper," Metallurgical and Materials Transactions A (Physical Metallurgy and Materials Science), 26A(11)(1995) 2881-2893.

13. L.E. Murr, M.A. Meyers, C.-S. Niou, Y.J. Chen, S. Pappu, and C. Kennedy, "Shock-Induced Deformation Twinning in Tantalum," Acta Metallurgica et Materialia, accepted (1996).

14. M.A. Meyers, Y.-J. Chen, F.D.S. Marquis, and D.S. Kim, "High-Strain, High-Strain-Rate Behavior of Tantalum," Metallurgical and Materials Transactions A (Physical Metallurgy and Materials Science), 26A(10)(1995) 2493-2501.

15. R.W. Armstrong, "The Influence of Polycrystal Grain Size on Mechanical Properties," Advances in Materials Research, 4, ed. Herbert Herman, (Wiley-Interscience, NY, 1971), 101-146.

16. F.J. Zerilli and R.W. Armstrong, "Description of Tantalum Deformation Behavior by Dislocation Mechanics Based Constitutive Relations," Journal of Applied Physics, 68(4)(1990) 1580-1591.

17. R. Vandermeer and W.B. Snyder, Jr., "Recovery and Recrystallization in Rolled Tantalum Single Crystals," Metallurgical Transactions A (Physical Metallurgy and Materials Science), 10A(8)(1979) 1031-1044.

18. T.E. Mitchell and W.A. Spitzig, "Three-Stage Hardening in Tantalum Single Crystals," Acta Metallurgica, 13 (1965) 1169-1179.

19. L.E. Malvern, Introduction to the Mechanics of a Continuous Medium, (Prentice-Hall, NJ, 1969), 364.

20. M.W. Chase Jr., C.A. Davies, J.R. Downey Jr., D.J. Frurip, R.A. McDonald, and A.N. Syverud, eds., JANAF Thermochemical Tables, Third Edition, Part II, Journal of Physical and Chemical Reference Data, Vol. 14, 1985, Supplement No. 1, (American Chemical Society and American Institute of Physics for the National Bureau of Standards, 1986), 1811.

21. W. Köck and P. Paschen, "Tantalum-Processing, Properties and Applications," Journal of Metals, 41(10)(1989) 33-39.

22. D. Beckenhauer, P. Niessen, and P. Pick, "Effect of Heating Rate on the Recrystallization Temperature of Tantalum," Journal of Materials Science Letters, 12(7)(1993) 449-450.

23. C.L. Wittman, R.K. Garrett, J.B. Clark, and C.M. Lopatin, "Defect Structures of Shocked Tantalum," Shock-Wave and High-Strain-Rate Phenomena in Materials, eds. M.A. Meyers, L.E. Murr, and K.P. Staudhammer, (M. Dekker, NY, 1992), 925.

24. J. Gil Sevillano, P. van Houtte, and E. Aernoudt, "Large Strain Work Hardening and Textures," Progress in Materials Science, 25(2-4)(1981) 69-409.

25. B. Derby, "The Dependence of Grain Size on Stress During Dynamic Recrystallization," Acta Metallurgica, 39(5)(1991) 955-962.

26. U. Andrade, M.A. Meyers, K.S. Vecchio, and A.H. Chokshi, "Dynamic Recrystallization in High-Strain, High-Strain-Rate Plastic Deformation of Copper," Acta Metallurgica et Materialia, 42(9)(1994) 3183-3195.

27. R.E. Reed-Hill, Physical Metallurgy Principles, 2nd ed., (Van Nostrand, NY, 1973), 304.

28. V.P. Krashchenko and V.E. Statsenko, Effect of Temperature and Strain-Rate in the Strength of Tantalum. I. Mechanical Properties," Strength of Materials, 13(2)(1981) 213-216.

29. D.R. Lide, ed., CRC Handbook of Chemistry and Physics, (CRC Press, Boston, 1990), 12-107.